Non-zero trilinear parameter in the mSUGRA model - dark matter and collider signals at Tevatron and LHC

Utpal Chattopadhyay[(a)1], Debottam Das[(a)2], Amitava Datta[(b)3] and Sujoy Poddar[(b)4]

[(a)] *Department of Theoretical Physics, Indian Association for the Cultivation of Science, Raja S.C. Mullick Road, Kolkata 700 032, India*

[(b)] *Department of Physics, Jadavpur University, Jadavpur, Kolkata 700 032, India*

Abstract

Phenomenologically viable and interesting regions of parameter space in the minimal super-gravity (mSUGRA) model with small m_0 and small $m_{1/2}$ consistent with the WMAP data on dark matter relic density and the bound on the mass of the lightest Higgs scalar $m_h > 114$ GeV from LEP2 open up if the rather adhoc assumption A_0=0, where A_0 is the common trilinear soft breaking parameter, employed in most of the existing analyses is relaxed. Since this region corresponds to relatively light squarks and gluinos which are likely to be probed extensively in the very early stages of the LHC experiments, the consequences of moderate or large negative values of A_0 are examined in detail. We find that in this region several processes including lightest supersymmetric particle (LSP) pair annihilation, LSP - lighter tau slepton ($\tilde{\tau}_1$) coannihilation and LSP - lighter top squark ($\tilde{t}_1$) coannihilation contribute to the observed dark matter relic density. The possibility that a $\tilde{t}_1$ that can participate in coannihilation with the lightest neutralino to satisfy the WMAP bound on relic density and at the same time be observed at the current experiments at the Tevatron is wide open. At the LHC a large number of squark - gluino events lead to a very distinctive semi-inclusive signature $\tau^{\pm}$+X$_\tau$ (anything without a tau lepton) with a characteristic size much larger than $e^{\pm}$+X$_e$ or $\mu^{\pm}$+X$_\mu$ events.

PACS no:04.65.+e,13.85.-t,14.80.Ly

[1]tpuc@iacs.res.in

[2]tpdd@iacs.res.in

[3]adatta@juphys.ernet.in

[4]sujoy@juphys.ernet.in

1 Introduction

Models with supersymmetry(SUSY)[1] are interesting for a variety of reasons. Theoretically the removal of quadratic divergence in the Higgs boson mass in the standard model (SM) by similar divergent loop diagrams involving SUSY particles (sparticles) is very attractive. These models have also predicted very interesting experimental signatures and are very promising candidates for beyond the standard model physics. A specially attractive feature of the minimal supersymmetric standard model (MSSM) with R-parity conservation is the presence of the stable, weakly interacting lightest neutralino ($\tilde{\chi}_1^0$) [2] which turns out to be a very good candidate for the observed cold dark matter (CDM) in the universe. [3, 4, 5].

Since superpartners are yet to be observed supersymmetry must be a broken symmetry and one requires a soft SUSY breaking mechanism that preserves gauge invariance and does not give rise to any quadratic divergence. The MSSM has a large number of such soft breaking parameters. Being guided by well motivated theoretical ideas as well as low energy phenomenology, models with specified SUSY breaking mechanisms drastically reduces the large number of such arbitrary parameters to only a few. The $N = 1$ supergravity models incorporate gravity mediated supersymmetry breaking and the models are attractive because of many features like gauge coupling unification, radiative breaking of electroweak symmetry [6], controlling flavour changing neutral currents (FCNC) by specific and simple assumptions at the unification scale [1].

The simplest gravity mediated SUSY breaking model - the minimal supergravity (mSUGRA)[7] model has only five free parameters. These are the common gaugino and scalar mass parameters $m_{1/2}$ and m_0, the common tri-linear coupling parameter A_0, all given at the gauge coupling unification scale ($M_G \sim 2 \times 10^{16}$ GeV), the ratio of Higgs vacuum expectation values at the electroweak scale namely $\tan\beta$ which is in fact largely independent of scale and the sign of μ, the higgsino mixing parameter. The magnitude of μ is obtained by the radiative electroweak symmetry breaking (REWSB) mechanism[6]. The low energy sparticle spectra and couplings at the electroweak scale are generated by renormalization group evolutions (RGE) of soft breaking masses and coupling parameters[8, 9].

Various SUSY models have been constrained by the data on cold dark matter relic density. But the recent resurgence of interest in this field is due to the very restrictive data from the Wilkinson Microwave Anisotropy Probe (WMAP) observation[10]. Combining the WMAP data with the results from the SDSS (Sloan Digital Sky Survey) one obtains the

conservative 3 σ limits

$$0.09 < \Omega_{CDM}h^2 < 0.13 \tag{1}$$

where $\Omega_{CDM}h^2$ is is the DM relic density in units of the critical density, $h = 0.71 \pm 0.026$ is the Hubble constant in units of 100 Km s^{-1} Mpc^{-1}. In supergravity type of models $\tilde{\chi}_1^0$ becomes the LSP for most of the parameter space[4, 5] and one may consider $\Omega_{CDM} \equiv \Omega_{\tilde{\chi}_1^0}$. We should note here that the upper bound of $\Omega_{\tilde{\chi}_1^0}$ in Eq.(1) is a strong limit but lower bound becomes weaker if we accept other candidates of dark matter.

In the thermally generated dark matter scenario, at very high temperature of the early universe ($T >> m_{\tilde{\chi}_1^0}$), $\tilde{\chi}_1^0$ was in thermal equilibrium with its annihilation products. The annihilation products include fermion pairs ($f\bar{f}$), gauge boson pairs (W^+W^- & ZZ), Higgs boson pairs ($hh, HH, AA, hH, hA, HA, H^+H^-$) or gauge boson-Higgs boson pairs (Zh, ZH, ZA & $W^\pm W^\mp$) through s, t and u channel diagrams. Thereafter, at lower temperatures the annihilation rate falls below the expansion rate of the universe and $\tilde{\chi}_1^0$ goes away from thermal equilibrium (freeze-out). The present value of the $\Omega_{\tilde{\chi}_1^0}h^2$ can thus be computed by solving the Boltzmann equation for $n_{\tilde{\chi}_1^0}$, the number density of the LSP in a Friedmann-Robertson-Walker universe. Finding the neutralino relic density most importantly involves computing the thermally averaged quantity $< \sigma_{eff}v >$, where v is the relative velocity between two neutralinos annihilating each other and σ_{eff} is the neutralino annihilation cross section which involves all possible final states. In addition to the annihilation of a LSP pair, coannihilations of the LSP [11, 12, 13, 14, 15] may also be important. This happens if there are sparticles with masses approximately degenerate with the LSP mass.

The annihilation cross section σ_{eff} depends on the magnitude of the bino ($\tilde{B}$),the wino ($\tilde{W}$) and the Higgsino ($\tilde{H}_1^0$, $\tilde{H}_2^0$) compositions of the lightest neutralino and proximity in mass of the LSP with any coannihilating sparticle. Generically the LSP composition is given by the following mixing:

$$\tilde{\chi}_1^0 = N_{11}\tilde{B} + N_{12}\tilde{W}_3 + N_{13}\tilde{H}_1^0 + N_{14}\tilde{H}_2^0. \tag{2}$$

Here the coefficients N_{ij} are the elements of the matrix that diagonalizes the neutralino mass matrix. One typically quantifies the composition through the gaugino fraction of $\tilde{\chi}_1^0$ which is defined as $F_g = |N_{11}|^2 + |N_{12}|^2$. A $\tilde{\chi}_1^0$ would be called gaugino like if F_g is very close to $1(\gtrsim 0.9)$, higgsino like if $F_g \lesssim 0.1$. Otherwise the LSP would be identified as a gaugino-higgsino mixed state.

Accordingly a typical MSSM parameter space (with gaugino mass universality) where the WMAP constraint is satisfied can be classified into several regions depending on the LSP annihilation/coannihilation mechanism. The list goes as follows.

i) In the so called *stau coannihilation* region, a large degree of $\tilde{\chi}_1^0 - \tilde{\tau}_1$ coannihilation[11] reduces the thermal abundance sufficiently so as to satisfy the WMAP data. The WMAP allowed region in the $m_0 - m_{1/2}$ plane in the mSUGRA model typically falls near the boundary of the forbidden parameter space where $\tilde{\tau}_1$ becomes the LSP. The coannihilation processes are of the type $\tilde{\chi}_1^0 \tilde{\ell}_R^a \to \ell^a \gamma, \ell^a Z, \ell^a h$, $\tilde{\ell}_R^a \tilde{\ell}_R^b \to \ell^a \ell^b$, and $\tilde{\ell}_R^a \tilde{\ell}_R^{b*} \to \ell^a \bar{\ell}^b, \gamma\gamma, \gamma Z, ZZ, W^+W^-, hh$. Here $\tilde{l}$ is essentially the $\tilde{\tau}_1$.

ii) The *focus point*[16] or the *Hyperbolic branch*[17] region in the mSUGRA model is characterized by a reduced value of $|\mu|$. A small $|\mu|$ causes the LSP to have a significant Higgsino component or it can even be a pure Higgsino. Strong coannihilation of the LSP with lighter chargino $\tilde{\chi}_1^\pm$ occurs in this zone. Some of the dominant coannihilation processes in these region are[13, 14]: $\tilde{\chi}_1^0 \tilde{\chi}_1^+, \tilde{\chi}_2^0 \tilde{\chi}_1^+ \to u_i \bar{d}_i, \bar{e}_i \nu_i, AW^+, ZW^+, W^+h$; $\tilde{\chi}_1^+ \tilde{\chi}_1^-, \tilde{\chi}_1^0 \tilde{\chi}_2^0 \to u_i \bar{u}_i, d_i \bar{d}_i, W^+W^-$. Having the smallest mass difference between coannihilating sparticles the process $\tilde{\chi}_1^0 \tilde{\chi}_1^+$ indeed dominates among the above channels. As a result the thermal abundance is reduced appreciably so that it satisfies the WMAP data or coannihilations may even reduce it further (below the lower limit of Eq.1) thus causing $\tilde{\chi}_1^0$ to be a sub dominant component of dark matter.

iii) The *funnel or the Higgs-pole* region[18, 19] satisfies the WMAP data for large values of $\tan\beta$ extending to both large m_0 and large $m_{1/2}$ regions. This is characterized by the direct-channel pole $2m_{\tilde{\chi}_1^0} \sim m_A, m_H$.

iv) For a limited range of large negative values of A_0, the lighter stop can become very light so that it may coannihilate with the LSP. This is the *stop coannihilation* region[12] characterized by a very light $m_{\tilde{t}_1}$.

v) In the *bulk annihilation region* or the bulk region[11] where m_0 and $m_{1/2}$ are reasonably small in mSUGRA, the LSP turns out to be bino dominated and, consequently, couples favourably to right sleptons, which in fact are the lightest sfermions in this region of parameter space. As a result an LSP pair annihilates into SM fermions via the exchange of light sfermions in the t-channel. This cross section depends on the mass of the LSP ($m_{\tilde{\chi}_1^0}$), its coupling with the sfermions and the masses of the exchanged sfermions [18, 4, 5]. However, LEP2 has imposed strong bounds on sparticle masses[20], particularly on the slepton masses

in the present context of mSUGRA and typical studies with $A_0 = 0$ disfavors a part of the bulk annihilation zone. Additionally, a very severe restriction appears on the $(m_0 - m_{1/2})$ plane of mSUGRA from the bound on lightest Higgs boson mass (m_h) [21] which practically rules out the entire annihilation region. For m_h >114 GeV one finds that within the frame work of mSUGRA the sleptons are significantly heavier than the direct LEP2 bounds and this leads to very small LSP annihilation cross section implying an unacceptably large relic density. Thus it has often been claimed in the recent literature that the mSUGRA parameter space with low values of both m_0 and $m_{1/2}$ is strongly disfavoured. This automatically eliminates the bulk annihilation region [22].

For small m_0 but relatively large $m_{1/2}$ one obtains a parameter space consistent with the Higgs mass bound. In this region a large $m_{1/2}$ pushes up the mass of the lightest neutralino while the lighter tau slepton $(\widetilde{\tau}_1)$ mass is rather modest because of a small m_0. Thus the LSP and $\widetilde{\tau}_1$ are approximately mass degenerate and LSP-$\widetilde{\tau}_1$ coannihilation [11] provides a viable mechanism of producing an acceptable relic density. However, the relatively large $m_{1/2}$ tends to push up the masses of squarks and gluino and this reduces the size of the LHC signals significantly.

The purpose of this paper is to emphasize that the above conclusions are artifacts of the adhoc choice $A_0 = 0$. Many of the current analyses invoke this choice without any compelling theoretical or experimental reason. On the other hand it is well known that moderate to large negative[5] values of A_0 lead to larger m_h[24]. Hence in this case the bound on m_h can be satisfied even for relatively small m_0 and small $m_{1/2}$. This revives the region where LSP pair annihilation is significant, which would otherwise remain forbidden for $A_0 = 0$ (see, e.g., LEPSUSY working group figures in Ref.[25]) [6]. Moreover the low $m_0 - m_{1/2}$ regions of the mSUGRA parameter space are characterized by relatively light squarks and gluino. Thus this region will be extensively probed at the early stages of the LHC experiments. It is therefore worthwhile to analyze the anticipated collider signals corresponding to this region in detail.

Even for moderate negative values of A_0 the WMAP allowed parameter space extends considerably. More importantly a small but interesting region where LSP pair annihilation

[5]We follow the standard sign convention of Ref.[23] for the signs of μ and A_0.

[6]For $A_0 > 0$, one requires m_0 and $m_{1/2}$ typically larger than the corresponding values for A_0=0. This does not lead to any novel collider signal.

produces an acceptable dark matter relic density is revived. There is also a region where LSP - $\widetilde{\tau}_1$ coannihilation is still the most important mechanism for having observed dark matter of the universe. Remarkably, even this region corresponds to a much smaller $m_{1/2}$ compared to what one would obtain for the A_0 =0 case. Consequently the squarks and gluinos become relatively lighter. Furthermore large negative values of A_0 leads to a relatively light top squark with obvious characteristics in the collider signals. In fact for a small region of the parameter space, the LSP- $\widetilde{t}_1$ coannihilation[12] may significantly contribute to the observed dark matter density.

In this paper emphasis will be given on the features of the sparticle spectrum and signals at the Tevatron and the LHC corresponding to the WMAP allowed regions of the parameter space opened up by non-zero A_0. Such signals will be compared and contrasted with the expectations from the scenarios with $A_0 = 0$.

Several earlier dark matter analyses considered non-zero trilinear couplings in various SUSY models including mSUGRA[26]. More recently it has also been noted in the literature [27] that the DM allowed mSUGRA parameter space is expanded for non-zero A_0 inspite of the constraint in Eq.1 and the lower bound on m_h from LEP2. However, in this work we go further and point out the dominant annihilation/co-annihilation mechanisms that would produce the acceptable amount of neutralino relic density in different regions and analyze the novel collider signals associated with them.

We have mainly considered the direct constraints from LEP2 searches and WMAP data on the mSUGRA parameter space. Other theoretical and experimental indirect constraints have also been considered in the literature. For example, it is well known that large values of A_0 may lead to a charge and colour breaking (CCB) minima[28]. We shall comment on it in the next section.

We note in passing that the constraints from the observed branching ratio BR($b- > s\gamma$)[29] disfavours the mSUGRA parameter space where both m_0 and $m_{1/2}$ happen to be small[22]. Parts of parameter space at the focus of attention of this paper belongs to this category. However, the theoretical prediction of this branching ratio in mSUGRA is based on the assumption of perfect alignment of the squark and quark mass matrices. This essentially means that the mixing angle factors at certain vertices (e.g., the quark-squark- gaugino vertices) are identical to the Cabibbo-Kobayashi-Maskawa (CKM) factors at the corresponding SM vartices. This assumption is unnecessarily restrictive and may be falsified by small off

diagonal terms in the squarks mass matrices at M_G which may change the mixing pattern in the squark sector drastically. It should be emphasized that the above small off diagonal entries do not affect the flavour conserving processes like neutralino annihilation or events at hadron colliders in any significant way. For a brief review of the model dependent assumptions in the $b- > s\gamma$ analyses we refer the reader to Okumura et al in [30] and Djouadi et al in [22].

2 The DM Allowed Parameter Space for Non-zero A_0 and the Sparticle Spectrum

In this section we relax the rather arbitrary choice $A_0 = 0$ and reexamine the scenarios with small m_0 and small $m_{1/2}$ consistent with the WMAP data. We remind ourselves that this particular region is strongly disfavored by the m_h bound from LEP2 for vanishing A_0.

We list the non-trivial consequences of considering a non-vanishing A_0. First, the lightest Higgs boson becomes heavier even if we choose a moderately negative value for A_0 keeping all other mSUGRA input parameters fixed. This happens via the mixing effects in the radiative corrections to m_h [24]. Moderately large negative values like $A_0 \approx -500$ GeV are adequate to satisfy the experimental lower bound on m_h even for small m_0 and small $m_{1/2}$.

However, three important additional effects should be taken into account while exploring the consequences of non-vanishing $A_0(< 0)$. i) With a negative A_0 having moderately large magnitude (thereby A_t - the trilinear coupling at the top quark sector at the weak scale being further negative), the lighter top squark $\tilde{t}_1$ will become much lighter than the other squarks because of the off-diagonal element $m_t(A_t - \mu \cot\beta)$ in the top squark mass matrix. In fact $\tilde{t}_1$ may even become the next lightest super particle (NLSP) or even violate the current experimental lower limit if A_t is sufficiently large and negative. We note here that unless $\tan\beta$ is very small, the amount of mixing in the $\tilde{t}_1$ sector is dominated by A_t in spite of the fact that $|\mu|$ determined by REWSB also becomes larger as A_0 is driven towards large negative values. ii) In the $\tilde{\tau}$ sector $\tilde{\tau}_1$ becomes lighter for large $|A_0|$ for entirely different reason. Here $\mu \tan\beta$ dominates over A_τ even for large $|A_0|$ and moderate $\tan\beta$. This pushes $\tilde{\tau}_1$ to become lighter. The effect of mixing is obviously larger for larger $\tan\beta$ or a larger $m_{1/2}$. As a result $\tilde{\tau}_1$ and to a lesser extent $\tilde{t}_1$ may become NLSP in different zones

of the parameter space around the bulk annihilation region. These two sparticles may thus coannihilate with the LSP and consistency with the WMAP limits on relic density may be obtained. iii) As mentioned in the introduction when $|A_0|$ becomes large one may hit a CCB minima of the scalar potential[28]. We have imposed the CCB conditions at the electroweak scale in this analysis. However these constraints can be altogether relaxed if it is assumed that the universe is built on the EWSB false vacuum with a life time larger than the age of the universe [31]. We therefore do not pursue these constraints at other scales.

In this analysis we have generated the electroweak scale sparticle spectrum from the input parameters at the unification scale by using the SuSpect code[32] with including the CCB condition as mentioned before. This code employs the two-loop renormalization group equations and implements the radiative electroweak symmetry breaking mechanism. We have used the code micrOMEGAs[33] for computing the neutralino relic density. We have included LEP2 lower limits for sparticle masses[20] and set top mass m_t =173 GeV. In particular the lower bound 94 GeV on $m_{\widetilde{\tau}_1}$ is quite important. However, we should also note here that the Higgs mass bound $m_h > 114$ GeV should be treated with caution. The theoretical prediction for the Higgs mass in the MSSM has been computed including two loop corrections[24]. It is well known that this prediction involves an uncertainty of about 3 GeV [34, 35, 36, 37, 38]. The sources of this uncertainty are the momentum-independent two-loop corrections, the momentum-dependent two-loop corrections, the higher loop corrections from t/$\widetilde{t}$ sector etc. While presenting the allowed parameter space we have , therefore, delineated the regions corresponding to 111 GeV $< m_h <$ 114 GeV. This parameter space which cannot be presently ruled out with certainty will be referred to as the uncertain m_h zone in this paper.

Additionally, we have randomly varied m_0 by 5 GeV around the quoted value of 120, 80 and 170 GeV in Fig.1, Fig.2 and Fig.3 respectively. We have introduced this variation since different spectrum generators do have small uncertainties in computing the sparticle masses in the mSUGRA framework. Similarly we have used a variation of 10 GeV for A_0 in Fig.4 around $A_0 = -700$ GeV.

We have also shown the consequences of the indirect constraint from the measured branching ratio of $b \to s\gamma$ [29, 30]. However as mentioned in the section.1 these constraint becomes weaker if some additional theoretical assumptions are dispensed with. We have used the constraint

$$2.77 \times 10^{-4} < Br(b \to s\gamma) < 4.33 \times 10^{-4} \tag{3}$$

at three sigma level.

Fig.(1(a)) shows different WMAP allowed zones in the $(A_0 - m_{1/2})$ plane for $\tan\beta = 10$, $m_0 = 120$ GeV. As mentioned before we have identified regions corresponding to 111 GeV $<$ $\mathrm{m_h} < 114$ GeV (the uncertain zone) and $m_h > 114$ GeV (the regular zone). We find WMAP allowed regions for small $m_{1/2}$ in both the zones. Additionally contours for $m_{\tilde{t}_1}$ are also shown. The WMAP allowed parameter space has three distinct regions.

1. In the region marked by the red dots the LSP pair annihilation is the dominant mechanism. However, this alone cannot satisfy the relic density constraint. Additional contributions come from a significant degree of LSP-$\tilde{t}_1$ coannihilation. As already mentioned this coannihilation is a direct consequence of a top squark NLSP with mass as low as $\sim$ 105 GeV due to large mixing effects in the top squark mass matrix for large and negative A_0. Such a light $m_{\tilde{t}_1}$ with $m_{\tilde{t}_1} - m_{\tilde{\chi}_1^0} \sim 30$ GeV is certainly within the striking range of Run II [39]. Thus if this scenario is indeed the one chosen by nature, the discovery of SUSY at LHC will be heralded by the discovery of the light top squark at the Tevatron.

2. In the region marked by the blue(deep shaded) dots neutralino pair annihilation is the main mechanism for satisfying the observed relic density. However there are points, the ones with relatively large $m_{1/2}$ in particular, where $\sim 50\%$ of the relic density is due to $\tilde{\tau}_1$-LSP coannihilation.

3. There is a third WMAP allowed region for larger $m_{1/2}$(the pink/light shaded dots).

   Here $\tilde{\tau}_1$-LSP coannihilation dominantes over LSP annihilation in satisfying the relic density. This coannihilation process becomes more and more effective as $m_{1/2}$ increases. However as noted before, in a scenario with REWSB, a moderately large negative A_0 yields large $|\mu|$. This causes $m_{\tilde{\tau}_1}$ to become smaller for smaller values of $m_{1/2}$ in comparison to the vanishing A_0 case. Thus larger $|A_0|$ may trigger $\tilde{\tau}_1$-LSP coannihilation at smaller values of $m_{1/2}$ which in turn predicts lighter squarks and gluinos in the WMAP allowed region.

The situation changes significantly if we change m_0 in either direction. Fig.(1(b)) illustrates the case of $m_0 = 80$ GeV. Here $|A_0|$ could not be as large as in the previous case

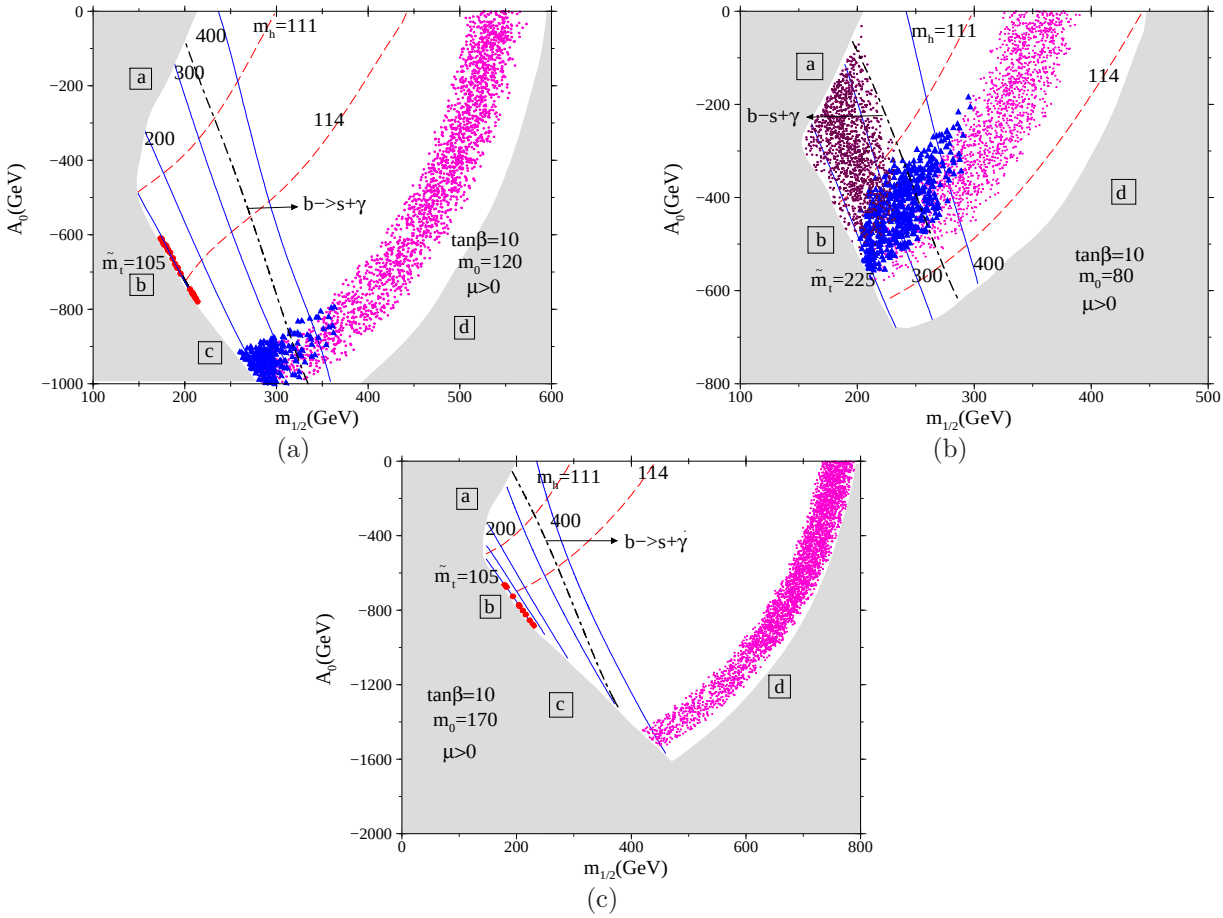

Figure 1: WMAP allowed region in the $m_{1/2} - A_0$ plane for $\tan\beta = 10$ and $m_0 = 120$, 80 and 170 GeV. Lighter stop masses are shown in (blue) solid lines. Dashed lines correspond to lighter Higgs masses. Dot-dashed lines refer to $b \to s\gamma$ limits. WMAP allowed zones: The brown(medium shaded) region near zone (a) refers to LSP pair annihilation. In the red region near zone (b) LSP pair annihilation and LSP-$\tilde{t}_1$ coannihilation jointly produce the relic density. The blue(deep shaded) region near zone (c) refers to a mixture of bulk annihilation and LSP-$\tilde{\tau}_1$ coannihilation. The pink(light shaded) region near zone (d) corresponds to a dominantly LSP-$\tilde{\tau}_1$ coannihilation. Disallowed zones: Region (a) is disallowed because either $\tilde{\chi}_1^{\pm}$ falls below the LEP limits or m_h becomes unacceptably small (< 108 GeV). Region (b) is ruled out by the lower limits on $m_{\tilde{t}_1}$ or/and $m_{\tilde{\tau}_1}$. Region (c) is disfavoured because CCB violating minima occurs at the elctroweak scale. Region (d) is discarded as $\tilde{\tau}_1$ becomes LSP.

Fig.(1(a)) because that would reduce $m_{\tilde{\tau}_1}$ below the experimental limit. This on the other hand does not allow any appreciable increase of m_h due to A_0. Smaller $|A_0|$ does not reduce $m_{\tilde{t}_1}$ appreciably so as to have any LSP-$\tilde{t}_1$ coannihilation. We note in passing that $m_{\tilde{t}_1} \leq 200$ GeV is disallowed since $\tilde{\tau}_1$ takes the charge of LSP here. This of course disfavours any LSP - $\tilde{t}_1$ coannihilation and $\tilde{t}_1$ is unlikely to be visible at the Tevatron [39].

The pure bulk region (shown in brown) is extended in comparison to the case of $m_0 =$ 120 GeV of Fig.(1(a)). However most of the extended parameter space corresponding to the bulk region has $m_h < 111$ GeV in this case. Additionally there is a sizable mixed region (where both LSP pair annihilation and LSP-$\tilde{\tau}_1$ coannihilation are important) which falls in the uncertain m_h zone.

On increasing m_0 to 170 GeV (Fig.(1(c))) we find no bulk annihilation region. Here negative and larger A_0 tends to reduce $m_{\tilde{\tau}_1}$, but a larger m_0 compensates. Thus $\tilde{t}_1$ may become the NLSP without having $\tilde{\tau}_1$ below $\tilde{\chi}_1^0$. As a consequence of such large A_0 one finds region with $m_h \geq$114. This scenario has a large LSP-$\tilde{\tau}_1$ coannihilation region (pink/light shaded dots) as well as a small LSP-$\tilde{t}_1$ coannihilation region (red dots). However, part of the LSP-$\tilde{\tau}_1$ coannihilation region is associated with significantly light squark/gluino masses compared to the $A_0 = 0$ case and such regions are well within the reach of the early probes at LHC.

Now we mention the status of the b$\rightarrow$ s γ constraint. The constraint disfavours the LSP-$\tilde{t}_1$ coannihilation region altogether in all the cases discussed above. But, segments of all three WMAP allowed regions are consistent with this constraint for $m_0 = 80$ GeV whereas a tiny part of mixed region and broad part of coannihilation region for $m_0 = 120$ GeV survive this constraint. On the other hand, for $m_0 = 170$ GeV the entire LSP- $\tilde{\tau}_1$ coannihilation region is allowed by this constraint. However, as mentioned in the section.1 the $b \rightarrow s\gamma$ constraint may loose much of its impact if additional theoretical assumptions like the alignment of the quark and the squark mass matrices are relaxed. We therefore prefer not to exclude any region allowed by the WMAP data on the basis of this constraint.

Fig.(2) shows the result for $\tan\beta = 5$. Here, allowed values of A_0 in Fig.(2) has a range larger than that of Fig.(1). The WMAP allowed regions for $m_0 = 120$ GeV Fig.(2(a)) consist of only coannihilations of LSP with $\tilde{t}_1$ and $\tilde{\tau}_1$ in contrast to the Fig.(1(a)) where a significant amount of mixed zone also exist. The dark matter satisfied parameter space for $m_0 = 80$ GeV of Fig.(2(b)) survives only if full allowance is made for the theoretical

uncertainty in the lighter Higgs mass calculation i.e the WMAP allowed region coincides with the uncertain m_h region. However, most of the region satisfy the $b \to s\gamma$ constraint of Eq.(3) except the pure bulk region and the LSP - $\tilde{t}_1$ coannihilation region. If this constraint is relaxed light top squarks within the striking range of Run II experiments are permitted. However, search for such light top squarks requires caution. For low $\tan\beta$ the branching ratio (BR) of the 4-body decay of this squark may be sizable or may even overwhelm the conventional loop decay[40]. Search strategies should be modified to include this usually neglected decay mode[41].

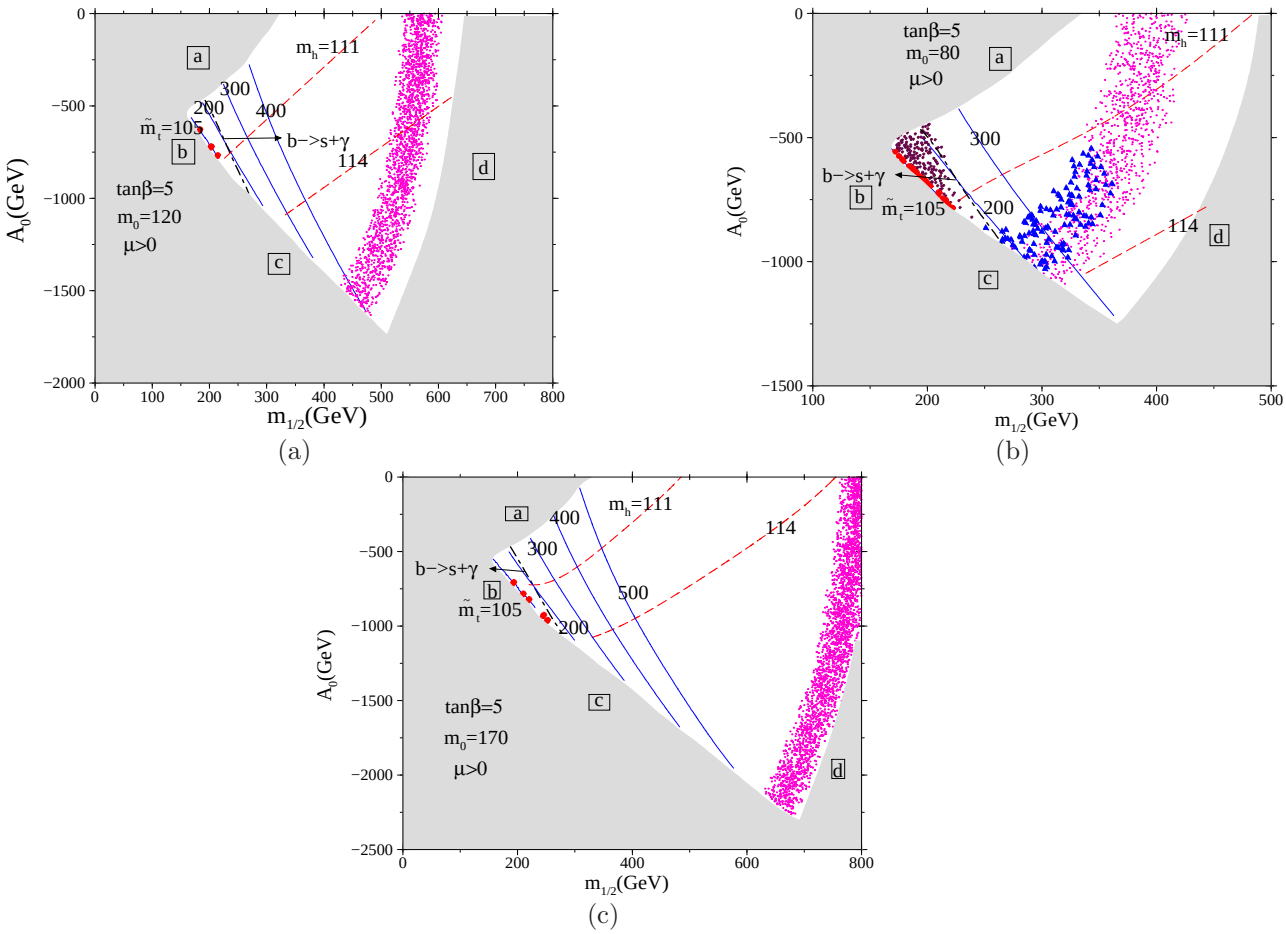

Figure 2: Same as Fig.1 except for $\tan\beta = 5$.

As an example of a large $\tan\beta$ case Fig.(3) shows the result for $\tan\beta = 30$ and $m_0 = 170$ GeV. Here the WMAP constraint is satisfied via LSP-$\tilde{\tau}_1$ coannihilation even if $m_h > 114$ GeV. One also obtains a mixed region where pair annihilation is the dominant mechanism. However this region corresponds to the uncertain m_h region i,e 111 GeV $< m_h <$ 114 GeV.

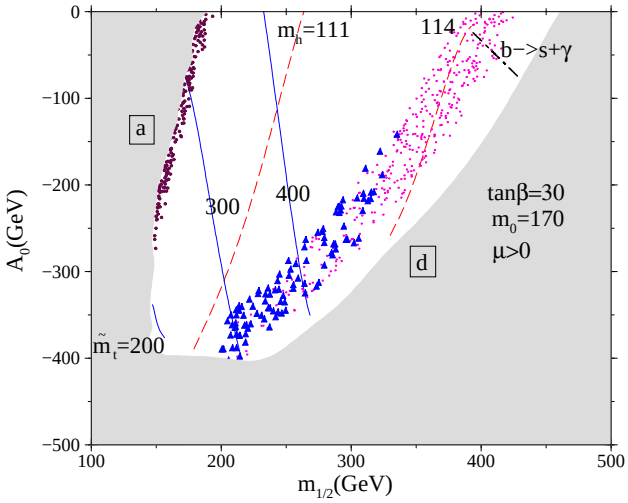

Figure 3: Same as Fig.1 except for $\tan\beta = 30$.

We next study the available parameter space in the m_0 - $m_{1/2}$ plane for a fixed negative value of $A_0 = -700$ GeV. As we see from Fig.(4) we get a pure bulk annihilation region, a mixed region as well as a $\tilde{\tau}_1$-LSP coannihilation region all satisfying the lighter Higgs bound and the WMAP limits. Additionally there is a significant region with LSP-$\tilde{t}_1$ coannihilation.

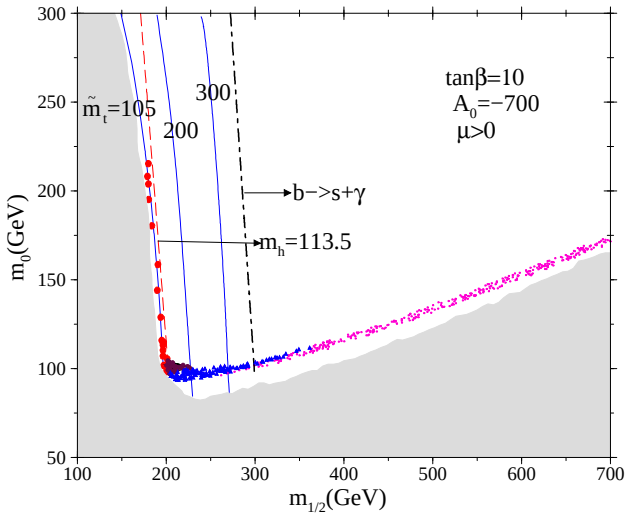

Figure 4: Same as Fig.1 except for being drawn in $m_0 - m_{1/2}$ plane for $\tan\beta = 10$ and $A_0 = -700$ GeV.

3 The Novel Collider Signals for non-zero values of the trilinear coupling

In this section we simulate all possible squark - gluino events using Pythia (version 6.409) [42] at the LHC energy ($\sqrt{s}$=14 TeV). We compute the relevant BRs using the program SDECAY [32]. From Fig (1(a)) we have chosen the following benchmark points as shown in Table 1.

A)This point corresponds to a mixed region where neutralino pair annihilation plays the dominant role. B)This point corresponds to the stau coannihilation region for a large negative value of A_0 and C) This point corresponds to the lowest value of $m_{1/2}$ in the LSP- $\tilde{\tau}_1$ coannihilation region for $A_0 = 0$.

mSUGRA parameters	A	B	C
m_0	120.0	120.0	120.0
$m_{1/2}$	300.0	350.0	500.0
A_0	-930.0	-930.0	0.0
$\tan\beta$	10.0	10.0	10.0
$sgn(\mu)$	1.0	1.0	1.0

Table 1: The three benchmark mSUGRA scenarios: (A): This parameter point with non-vanishing A_0 belongs to a mixed region characterized by LSP pair annihilation and LSP-$\tilde{\tau}_1$ coannihilation, (B): This point with non-vanishing A_0 belongs to a region where stau coannihilation dominates among the annihilation/coannihilation processes, (C) This point with vanishing A_0 refers to the lowest value of $m_{1/2}$ in the LSP-$\tilde{\tau}_1$ coannihilation region. All parameters with dimensions of mass are in GeV.

The sparticle spectra for the three benchmark points are shown in Table 2. Table 3 shows the branching ratios of the dominant decay modes of gluino and for the squarks of the first two generations. The branching ratios of the third generation of squarks are shown in Table 4. We have further computed the branching ratios of the dominant decay modes of

the lighter chargino and the second lightest neutralino. The result is shown in Table 5.

Squark/ Slepton/Gluino/ Gaugino masses	A	B	C
$\widetilde{g}$	719.0	827.0	1149.0
$\widetilde{q}_L$	670.0	769.0	1055.0
$\widetilde{q}_R$	647.0	739.0	1015.0
$\widetilde{t}_1$	286.0	396.0	807.0
$\widetilde{t}_2$	644.0	728.0	1016.0
$\widetilde{b}_1$	558.0	652.0	974.0
$\widetilde{b}_2$	639.0	731.0	1009.0
$\widetilde{l}_L$	239.0	268.0	355.0
$\widetilde{\nu}_{l_L}$	226.0	255.0	346.0
$\widetilde{l}_R$	169.0	182.0	224.0
$\widetilde{\tau}_1$	132.0	148.0	217.0
$\widetilde{\nu}_{\tau_L}$	218.0	248.0	345.0
$\widetilde{\tau}_2$	241.0	268.0	357.0
$\widetilde{\chi}_1^{\pm}$	232.0	272.0	386.0
$\widetilde{\chi}_2^{\pm}$	616.0	669.0	649.0
$\widetilde{\chi}_1^0$	121.0	142.0	205.0
$\widetilde{\chi}_2^0$	232.0	272.0	386.0
h	117.0	117.0	115.0

Table 2: The sparticle spectra in the three scenarios. All masses are in GeV.

Next we present the total squark-gluino production cross-sections for the three scenarios in Table 6. These lowest order cross sections have been computed by CalcHEP (version 2.3.7)[43]. From this table it is obvious that even for 10 fb^{-1} of integrated luminosity scenario A) will produce a remarkably large number of squark-gluino events compared to the other two scenarios. Thus it can be easily tested by the early LHC runs. On the otherhand if $\tilde{\chi}_1^0$ - $\tilde{\tau}_1$ coannihilation happens to be the dominant mechanism for obtaining the present day

Decay modes (squark/gluino)	A %	B %	C %
$\widetilde{g} \to \widetilde{q}_L q$	8.8	10.4	18.0
$\widetilde{g} \to \widetilde{q}_R q$	18.4	21.2	35.2
$\widetilde{g} \to \widetilde{b}_1 b$	19.4	18.6	13.8
$\widetilde{g} \to \widetilde{b}_2 b$	5.6	6.4	9.4
$\widetilde{g} \to \widetilde{t}_1 t$	47.0	43.0	23.0
$\widetilde{q}_L \to \widetilde{\chi}_1^+ q$	66.0	66.0	64.6
$\widetilde{q}_L \to \widetilde{\chi}_2^0 q$	32.6	32.8	32.0
$\widetilde{q}_R \to \widetilde{\chi}_1^0 q$	100.0	100.0	100.0

Table 3: The BRs (%) of the dominant decay modes of the gluinos and the squarks belonging to the first two generations.

thermal abundance and A_0 is large negative (scenario B), the size of the signal may still be more than an order of magnitude larger than what is expected in scenario C)corresponding to $A_0 = 0$. The relative sizes of the total cross sections in the three cases can be qualitatively understood from the sparticle spectra as shown in Table 2.

We next turn to some distinctive features of the signals from the three scenarios. This criteria may be utilized as a confirmation of the underlying SUSY scenarios that correspond to different mechanisms of neutralino annihilation for an acceptable relic density. From the decay tables it is evident that the signals from decaying sparticles in A) and B) will contain many more tau-leptons than electrons or muons showing thereby a strong departure from "lepton universality". However, in scenario C) this universality in the signal will hold approximately.

The main reason for this "non-universality" lies in the dominant 2 - body decay modes of $\widetilde{\chi}_1^\pm$ and $\widetilde{\chi}_2^0$. It is to be noted that in scenario A) the $\widetilde{\chi}_1^\pm$ decays into the lighter stau(with a dominant $\widetilde{\tau}_R$ component) with a large BR. This is due to the fact that the lighter charginos can decay only into right handed sleptons via two body modes. However this decay is allowed only through the small higgsino component of the gaugino like chargino. Thus the decay into $\widetilde{\tau}_1$ dominates. Again since $\widetilde{\nu}_\tau$ is lighter than the other sneutrinos, $\widetilde{\chi}_1^\pm$ decays into $\widetilde{\nu}_\tau$

Decay modes (heavy squark)	A %	B %	C %
$\widetilde{b}_1 \to \widetilde{\chi}_2^0 b$	12.0	14.0	19.7
$\widetilde{b}_1 \to \widetilde{\chi}_1^- t$	16.0	21.5	35.0
$\widetilde{b}_1 \to \widetilde{t}_1 W^-$	70.0	63.4	13.0
$\widetilde{b}_1 \to \widetilde{\chi}_2^- t$	0.0	0.0	29.0
$\widetilde{t}_1 \to \widetilde{\chi}_1^- b$	100.0	49.0	36.0
$\widetilde{t}_1 \to \widetilde{\chi}_1^0 t$	0.0	51.0	29.0
$\widetilde{t}_1 \to \widetilde{\chi}_2^0 t$	0.0	0.0	14.0
$\widetilde{b}_2 \to \widetilde{\chi}_1^0 b$	28.4	3.3	24.5
$\widetilde{b}_2 \to \widetilde{\chi}_2^0 b$	3.9	4.2	6.7
$\widetilde{b}_2 \to \widetilde{\chi}_1^- t$	5.9	6.9	12.0
$\widetilde{b}_2 \to \widetilde{t}_1 W^-$	61.0	54.0	13.0

Table 4: The BRs (%) of the dominant decay modes of the squarks belonging to the third generation.

and tau with a sizable BR. In all three scenarios the sneutrino decays invisibly via the mode $\tilde{\nu}_i \to \nu_i + \tilde{\chi}_1^0$ (i=e, μ, τ). Thus the second lightest neutralino dominantly decays either into invisible neutrino-sneutrino pairs or into τ and $\widetilde{\tau}_1$ with large BRs. As a result there is a significantly large tau excess in the semi-inclusive signal $\tau^{\pm}$+X$_\tau$, (where X$_\tau$ stands all final states without a tau) compared to $e^{\pm}$+X$_e$ or $\mu^{\pm}$+X$_\mu$.

In the squark gluino events $\widetilde{\chi}_1^{\pm}$ and $\widetilde{\chi}_2^0$ primarily arise from the decays of $\widetilde{q}_L$ and $\widetilde{t}_1$ decays into $\widetilde{\chi}_1^{\pm}$ and b with 100% BR. Moreover since $\widetilde{t}_1$ is much lighter compared to the other squarks due to the large magnitude of the A_0 parameter the gluinos decay into $\widetilde{t}_1 - t$ pairs with a large BR.

Scenario B) has all the above features albeit to a lesser extent. It is particularly important to note that more than 50% of the $\widetilde{t}_1$s decays into $t - \widetilde{\chi}_1^0$ pairs. The decays of the t tend to restore lepton universality. Thus the excess of events with τ leptons over the ones with e or μ is reduced to some extent.

In scenario C) the excess of tau leptons is reduced drastically as is evident from decay

Decay modes (Gauginos)	A %	B %	C %
$\widetilde{\chi}_2^0 \to \widetilde{\tau}_1^+ \tau^-$	78.6	46.0	8.4
$\widetilde{\chi}_2^0 \to \widetilde{\nu}_l \nu_l$	5.2	24.0	33.8
$\widetilde{\chi}_2^0 \to \widetilde{\nu}_\tau \nu_\tau$	15.0	24.0	17.8
$\widetilde{\chi}_1^+ \to \widetilde{\chi}_1^0 W^+$	2.6	2.6	5.1
$\widetilde{\chi}_1^+ \to \widetilde{\nu}_l l^+$	5.4	25.0	36.0
$\widetilde{\chi}_1^+ \to \widetilde{\nu}_\tau \tau^+$	16.0	25.0	19.2
$\widetilde{\chi}_1^+ \to \widetilde{\tau}_1^+ \nu_\tau$	76.0	44.0	7.9

Table 5: The BRs (%) of the dominant decay modes of the lighter chargino and the second lightest neutralino. All sneutrinos decay into the invisible channel $\nu + \widetilde{\chi}_1^0$ in the three cases under study.

tables.

However, it must be borne in mind that the decays of the standard model particles (mainly t, Z and W) present in the signal exhibit lepton universality. Moreover, the heavy flavour (b, c, t) decays yield more electrons and muons than taus. It is therefore essential to calculate the relative abundance of different charged leptons in the signal through simplified simulations.

To begin with we ignore the difference in the detection efficiencies of different leptons. This will be addressed later in the paper. Again the production and decay of all squark-gluino pairs are generated by Pythia. In this simplified parton level analysis all SM particles other than the W, Z and t are treated as stable. All unstable sparticles are allowed to decay. Hadronization, fragmentation and jet formation are switched off. We also impose the cuts $p_T > 30.0$ GeV and $|\eta_l| < 2.5$ on e, μ and τ. This is to have a feeling for the numbers when e's and the μ's in the final state from b and c decays are minimized (see the improved analysis presented below). The results are shown in Table 7. In this table the first row corresponds to the number of semi-inclusive events with only one τ. The second and third rows give the corresponding numbers for final states with one e and one μ respectively.

From Table 7 it is obvious that in scenario A) the number of events with only one τ is

Process	σ(pb)		
	A	B	C
$\widetilde{g}\widetilde{g}$	1.41	0.55	0.05
$\widetilde{q}_L\widetilde{g}$	2.35	1.08	0.15
$\widetilde{q}_R\widetilde{g}$	2.55	1.18	0.16
$\widetilde{q}_L\widetilde{q}_L$	0.78	0.55	0.13
$\widetilde{q}_L\widetilde{q}_L^*$	0.18	0.08	0.01
$\widetilde{q}_R\widetilde{q}_R$	0.75	0.47	0.11
$\widetilde{q}_R\widetilde{q}_R^*$	0.22	0.10	0.01
$\widetilde{q}_L\widetilde{q}_R$	0.47	0.25	0.05
$\widetilde{q}_L\widetilde{q}_R^* + c.c$	0.43	0.21	0.04
$\widetilde{t}_1\widetilde{t}_1^*$	6.12	1.14	0.02
$\widetilde{t}_2\widetilde{t}_2^*$	0.07	0.03	0.004
$\widetilde{t}_1\widetilde{t}_2^* + c.c$	0.001	0.0002	1.5×10^{-5}
$\widetilde{b}_1\widetilde{b}_1^*$	0.17	0.07	0.005
$\widetilde{b}_2\widetilde{b}_2^*$	0.08	0.03	0.004
Total	15.58	5.74	0.74

Table 6: The production cross sections of all squark-gluino events studied in this paper.

much larger than the corresponding events with e or μ. The excess of events involving only one τ lepton is also seen in scenario B). The scenario C) exhibits lepton universality.

Since the gluinos dominantly decay into b or t flavoured squarks in scenarios A) and B) we expect a sizable number of b quarks in the final state. This is also illustrated in Table 7 (see the last five rows).

Thus in principle b-tagging may be effectively used to suppress the backgrounds except the ones from $t-\bar{t}$ production.

To demonstrate that the above tau excess survives the typical kinematical cuts designed for SUSY search experiments at the LHC we proceed as follows. Since a detailed background simulation is beyond the scope of this paper we apply a slightly modified version of the generic cuts introduced by the ATLAS collaboration to eliminate the SM backgrounds in their study of inclusive SUSY signals [44]. We shall, however, study the response of the $t-\bar{t}$ events,

	A	B	C
$1\tau + X_\tau$	29870	11860	1340
$1\mu + X_\mu$	5274	4251	1260
$1e + X_e$	5294	4232	1262
$1\tau + 0b + X_\tau$	10750	4581	747
$1\tau + 1b + X_\tau$	19	13	1
$1\tau + 2b + X_\tau$	17099	6589	507
$1\tau + 3b + X_\tau$	9	6	0
$1\tau + 4b + X_\tau$	425	665	80

Table 7: The number of semi-inclusive events with one τ, one e and one μ at the parton level. X stands for all possible final states excluding the lepton indicated by the subscript. The last five rows indicate the number of b quarks in the τ type events. All numbers correspond to an integrated luminosity of 10 fb^{-1}.

	A	B	C	$t\bar{t}$
$1\tau + X_\tau$	3113	1402	239	481
$1\mu + X_\mu$	1179	1246	820	1295
$1e + X_e$	1138	1263	829	1354

Table 8: The number of semi-inclusive events with one detected τ jet, one isolated e and one isolated μ computed by Pythia. The selection criteria and the kinematical cuts are given the text. The last column gives the contributions of the background from $t - \bar{t}$ production.

likely to be the dominant SM background, to these cuts after our signal analysis.

Again all squark-gluino events are generated by Pythia. Initial and final state radiation, decay, hadronization, fragmentation and jet formation are implemented following the standard procedures in Pythia. We impose the following selection and background rejection criterion:

1. Only jets having transverse energy $E_T^j > 30$ GeV, pseudo rapidity $|\eta_j| < 4.5$ and the

jet-jet isolation parameter $\Delta R(j_1, j_2) > 0.5$ are selected from the toy calorimeter of Pythia.

2. The jets arising from hadronic tau decays are selected as follows. Firstly τ's having transverse momentum $p_T > 20$ GeV and pseudo rapidity $|\eta_\tau| < 3$ are identified. These τs are matched with the jets by setting the following criterion $\Delta R(\tau, j) < 0.4$ and $E_T^j/E_T^\tau > 0.8$, where E_T^j is the transverse energy of jets and E_T^τ is the same for the τ being matched. The possibility of detecting the matched τs is then computed using the detection efficiencies in [45](see Fig 12.9, p 444 in section 12.1.2.2).

3. We also require that an isolated e or μ in an event have $p_T > 30$ GeV and the lepton-jet isolation parameter $\Delta R(l, j) > 0.5$, where l stands for either e or μ. The detection efficiencies of these leptons are assumed to be 100%.

4. We reject events without at least two jets having transverse momentum $P_T > 150$ GeV.

5. Events are rejected if missing transverse energy $\not{E}_T < 200$ GeV.

6. Only events with jets having $S_T > 0.2$, where S_T is a standard function of the eigen values of the sphericity tensor, are accepted.

The strong p_T and isolation criteria on e and μ enable us to exclude the most of leptons from semileptonic b and c decays from the list of isolated leptons in an event. We have checked that a suitable cut on M_{eff}, where $M_{eff} = |\not{E}_T| + \Sigma_{i=1}^2 |p_T^{l_i}| + \Sigma_{i=1}^4 |p_T^{j_i}|$ $(l = e, \mu)$ does not improve the ratio $S/\sqrt{B}$ significantly, where S corresponds to number of signal events and B represents the number of background events.

We present the number of semi-inclusive events with only one detected τ jet, with only one isolated μ or e in Table 8. The number of events corresponds to an integrated luminosity of 10 fb^{-1}. It is clear from the table that inspite of non-ideal τ detection efficiencies there is indeed an excess of events with tau leptons over that with electrons and muons in scenario A). In scenario B) the number of events with tau leptons is reduced as expected compared to A) but is still significantly larger than the corresponding number in C).

We note in passing that there are several proposals for detecting the taus [45]. The combined efficiency may be larger than the efficiency obtained from tracker isolation alone which we have used. However, the combined efficiency is process dependent [45]and in this

simplified analysis we have not employed it. Also following the CMS guidelines we have not considered the possibility of detecting tau-jets with $p_T < 30$ GeV. However, we have noted that a large number of tau-jets in the final state have p_T in this region. If future works establish the techniques of detecting these relatively low p_T tau jets, the excess of final states involving τs will be even more dramatic.

We next study the dominant background from $t - \bar{t}$ events using the selection criteria and kinematical cuts given above. The leading order cross-section for this process computed by CalcHEP is 400 pb.

The results are given in the last column of Table 8. The $S/\sqrt{B}$ ratios in the three scenarios indicate that statistically significant signals are expected in all cases. Since b-tagging is not particularly helpful in rejecting this particular background we have not incorporated it here. However in a more complete background analysis b-tagging may indeed be a useful tool as our parton level analysis indicates.

As noted in the introduction a consequence of large negative A_0 is the possibility of a light top squark which can be as light as the 105 GeV (Fig.1 - 4). For such a light $\widetilde{t}_1$ its coannihilation with the LSP may be one of the important mechanisms for having the observed DM in the universe. Moreover, the LSP mass in this region of the parameter space is about 25-30 GeV lesser than $m_{\tilde{t}_1}$. Hence, the top squark NLSP will decay via the loop mediated mode $c+\widetilde{\chi}_1^0$ with 100 % BR. The prospect of light stop squark search in this channel at Tevatron Run II was studied in [39]. If this scenario for thermal abundance of dark matter in the universe is realized in nature SUSY search at LHC will certainly be heralded by the discovery of $\widetilde{t}_1$ at the Tevatron. Even in scenario B) the $\widetilde{t}_1$ will be considerably lighter compared to scenario C) (see Table 2) although its mass will still be outside the kinematic reach of the Tevatron. However this squark will have a sizable production cross section at the LHC. Hence its discovery may be an additional confirmation of a mechanism of producing an acceptable DM relic density based on $\tilde{\chi}_1^0$ - $\tilde{t}_1$ coannihilation with large negative A_0.

An additional feature of WMAP allowed regions of the parameter space with low m_0 is the existence of sneutrinos decaying invisibly. This happens in all three scenarios A, B and C. Moreover, the $\widetilde{\chi}_2^0$ decays into sneutrino neutrino pairs with sizable BR. Thus in addition to the LSP there are two other carriers of missing energy. An important consequence of these scenarios is the spectacular enhancement of the signal $e^+e^- \to \gamma$ + missing energy over the SM background from $e^+e^- \to \nu_i\bar{\nu}_i + \gamma$ (i=e, μ, τ). The signal comes from three channels

$e^+e^- \rightarrow \tilde{\chi}_1^0\tilde{\chi}_1^0\gamma$,$\tilde{\chi}_2^0\tilde{\chi}_2^0\gamma$, $\tilde{\nu}\tilde{\nu}^\star\gamma$. The signal from the first SUSY process was computed in [46] with the approximation that $\tilde{\chi}_1^0$ is a pure photino. All three cross-sections including the effect of neutralino mixing were computed in [47]. The results of [47] were compared with that of CalcHEP in [48]. The observation of the signal at the ILC may provide additional confirmation of SUSY dark matter if produced in the low $m_0, m_{1/2}$ region of the mSUGRA model.

4 Conclusions

In this work we observe that parts of the low m_0 - $m_{1/2}$ region of the mSUGRA model with moderate or large negative values of the common trilinear coupling A_0 at M_G are consistent with the current direct bounds on sparticle masses from LEP as well as the WMAP bound on the dark matter relic density (Fig.1 - 4). In particular the LEP bound m_h >114 GeV can be easily satisfied for relatively small m_0 and $m_{1/2}$ if A_0 is large and negative (Fig.1 - 4). This possibility is excluded by the adhoc choice A_0 =0 made in many current analyses.

The relic density is produced by several processes including LSP - pair annihilation, LSP - $\tilde{t}_1$ or LSP - $\tilde{\tau}_1$ coannihilation or by suitable combinations of these processes.

This parameter space corresponding to relatively light squarks and light gluinos is important since it will be extensively scanned at the early runs of the LHC. A large excess of semi-inclusive events of the type $\tau^\pm$+X$_\tau$ (see Tables 7 and 8) over $e^\pm$+X$_e$ or $\mu^\pm$+X$_\mu$ events is a hallmark of scenarios with large negative A_0 in mSUGRA. Our simulations with three bench-mark scenarios (see Table 1) consistent with direct lower bounds on sparticle masses and WMAP data establish this for a modest integrated luminosity of 10 fb^{-1}.

A natural consequence of large negative A_0 is a light $\tilde{t}_1$. If that be the case then $\tilde{t}_1$ - $\tilde{\chi}_1^0$ coannihilation may be an important mechanism for the present day dark matter density. In this scenario the discovery of SUSY at the LHC is likely to be preceded by the discovery of $\tilde{t}_1$ at the Tevatron.

Several groups have also imposed indirect constraints on the allowed parameter space [22]. However, it is well known that each of these indirect constraints employ additional theoretical assumptions which are not fool proof. For example the requirement that there be no CCB minima of the scalar potential deeper than the EWSB vacuum [28] becomes redundant if the latter is assumed to be a false vacuum with a life time larger than the

age of the universe [31]. Similarly the constraint from the measured branching ratio of the decay $b \to s\gamma$ derived under the purely theoretical assumption that quark and squark mass matrices are perfectly aligned can also be evaded if this assumption is relaxed (see,e.g., Djouadi et al in [22]and references therein). Although we have shown the consequences of some of these indirect bounds in our figures it may not be prudent to discard any parameter space if these bounds are violated.

Acknowledgment: AD acknowledges financial support from the Department of Science and Technology, Government of India under the project No (SR/S2/HEP-18/2003). SP and DD would like to thank the Council of Scientific and Industrial Research, Govt. of India for financial support.

References

[1] For reviews on Supersymmetry, see, *e.g.* , H. P. Nilles, Phys. Rep. **110**, 1 (1984); H. E. Haber and G. Kane, Phys. Rep. **117**, 75 (1985) ; J. Wess and J. Bagger, *Supersymmetry and Supergravity*, 2nd ed., (Princeton, 1991); M. Drees, P. Roy and R. M. Godbole, *Theory and Phenomenology of Sparticles*, (World Scientific, Singapore, 2005).

[2] H. Goldberg, Phys. Rev. Lett. **50**, 1419 (1983); J. Ellis, J. Hagelin, D. Nanopoulos and M. Srednicki, Phys. Lett. **B127**, 233 (1983); J. Ellis, J. Hagelin, D. Nanopoulos, K. Olive and M. Srednicki, Nucl. Phys. **B238**, 453 (1984).

[3] G. Bertone, D. Hooper and J. Silk, Phys. Rept. **405**, 279 (2005), [arXiv:hep-ph/0404175]; W. L. Freedman and M. S. Turner, Rev. Mod. Phys. **75**, 1433 (2003), [arXiv:astro-ph/0308418]; L. Roszkowski, Pramana **62**, 389 (2004), [arXiv:hep-ph/0404052].

[4] G. Jungman, M. Kamionkowski and K.Greist, Phys. Rep. **267**,195(1996).

[5] A. B. Lahanas, N. E. Mavromatos and D. V. Nanopoulos, Int. J. Mod. Phys. D **12**, 1529 (2003) [arXiv:hep-ph/0308251]; C. Munoz, Int. J. Mod. Phys. A **19**, 3093 (2004) [arXiv:hep-ph/0309346]; Manuel Drees, Plenary talk at 11th International Symposium

on Particles, Strings and Cosmology (PASCOS 2005), Gyeongju, Korea, 30 May - 4 Jun 2005 (published in AIP Conf.Proc., **805**, 48-54, (2006).

[6] L. E. Ibanez and G. G. Ross, Phys. Lett. B **110**, 215 (1982); K. Inoue, A. Kakuto, H. Komatsu and S. Takeshita, Prog. Theor. Phys. **68**, 927 (1982) [Erratum-ibid. **70**, 330 (1983)]; J. R. Ellis, J. S. Hagelin, D. V. Nanopoulos and K. Tamvakis, Phys. Lett. B **125**, 275 (1983); L. Alvarez-Gaume, J. Polchinski and M. B. Wise, Nucl. Phys. B **221**, 495 (1983).

[7] A. H. Chamseddine, R. Arnowitt and P. Nath, Phys. Rev. Lett. **49**, 970 (1982); R. Barbieri, S. Ferrara and C. A. Savoy, Phys. Lett. B **119**, 343 (1982); L. J. Hall, J. Lykken and S. Weinberg, Phys. Rev. D **27**, 2359 (1983); P. Nath, R. Arnowitt and A. H. Chamseddine, Nucl. Phys. B **227**, 121 (1983); N. Ohta, Prog. Theor. Phys. **70**, 542 (1983); For reviews see [1] and P. Nath, R. Arnowitt and A.H. Chamseddine, *Applied N =1 Supergravity* (World Scientific, Singapore, 1984).

[8] M. E. Machacek and M. T. Vaughn, Nucl. Phys. B **222**, 83 (1983); Nucl. Phys. B **236**, 221 (1984); Nucl. Phys. B **249**, 70 (1985).

[9] S. P. Martin and M. T. Vaughn, Phys. Lett. B **318**, 331 (1993) [arXiv:hep-ph/9308222]; Phys. Rev. D **50**, 2282 (1994) [arXiv:hep-ph/9311340]; I. Jack, D. R. Jones, S. P. Martin, M. T. Vaughn and Y. Yamada, Phys. Rev. D **50**, 5481 (1994) [arXiv:hep-ph/9407291].

[10] D. N. Spergel *et al.*, arXiv:astro-ph/0603449.

[11] J. R. Ellis, T. Falk and K. A. Olive, Phys. Lett. B **444**, 367 (1998); J. R. Ellis, T. Falk, K. A. Olive and M. Srednicki, Astropart. Phys. **13**, 181 (2000) [Erratum-ibid. **15**, 413 (2001)]; A. Lahanas, D. V. Nanopoulos and V. Spanos, Phys. Rev. D **62**, 023515 (2000); R. Arnowitt, B. Dutta and Y. Santoso, Nucl. Phys. B **606**, 59(2001); T. Nihei, L. Roszkowski and R. Ruiz de Austri, JHEP **0207**, 024 (2002); V. A. Bednyakov, H. V. Klapdor-Kleingrothaus and V. Gronewold, Phys. Rev. D **66**, 115005 (2002).

[12] C. Boehm, A. Djouadi and Manuel Drees, Phys. Rev. D **62**, 035012(2000); J. R. Ellis, K. A. Olive and Y. Santoso, Astropart. Phys. **18**, 395 (2003).

[13] J. Edsjo and P. Gondolo, Phys. Rev. D **56**, 1879 (1997).

[14] S. Mizuta and M. Yamaguchi, Phys. Lett. B **298**, 120 (1993) [arXiv:hep-ph/9208251].

[15] R. Arnowitt, B. Dutta and Y. Santoso, Nucl. Phys. B **606**, 59 (2001); V. A. Bednyakov, H. V. Klapdor-Kleingrothaus and V. Gronewold, arXiv:hep-ph/0208178.

[16] J. L. Feng, K. T. Matchev and T. Moroi, Phys. Rev. D **61**, 075005 (2000); Phys. Rev. Lett. **84**, 2322 (2000); J. L. Feng, K. T. Matchev and F. Wilczek, Phys. Lett. B **482**, 388 (2000); J. L. Feng and F. Wilczek, Phys. Lett. B **631**, 170 (2005) [arXiv:hep-ph/0507032].

[17] K. L. Chan, U. Chattopadhyay and P. Nath, Phys. Rev. D **58**, 096004 (1998); [arXiv:hep-ph/9710473]; U. Chattopadhyay, A. Corsetti and P. Nath, Phys. Rev. D **68**, 035005 (2003) [arXiv:hep-ph/0303201].

[18] M. Drees and M. Nojiri, Phys. Rev. **D47**, 376 (1993).

[19] R. Arnowitt and P. Nath, Phys. Rev. Lett. **70**, 3696 (1993); H. Baer and M. Brhlik, Phys. Rev. **D53**, 597 (1996), Phys. Rev. D **57**, 567 (1998); H. Baer, M. Brhlik, M. Diaz, J. Ferrandis, P. Mercadante, P. Quintana and X. Tata, Phys. Rev. **D63**, 015007 (2001); J. R. Ellis, T. Falk, G. Ganis, K. A. Olive and M. Srednicki, Phys. Lett. B **510**, 236 (2001); A. B. Lahanas and V. C. Spanos, Eur. Phys. J. C **23**, 185 (2002); A. Djouadi, M. Drees and J. Kneur, Phys. Lett. B **624** 60 (2005).

[20] For the latest limits on the sparticle masses from LEP experiments: see http://lepsusy.web.cern.ch/lepsusy/

[21] R. Barate *et al.* [LEP Working Group for Higgs boson searches], Phys. Lett. B **565**, 61 (2003) [arXiv:hep-ex/0306033].

[22] J. R. Ellis, K. A. Olive and Y. Santoso, New J. Phys. **4**, 32 (2002) J. Ellis, K. Olive, Y. Santoso and V. Spanos, Phys. Lett. B **565** 176 (2003); H. Baer and C. Balazs, JCAP **0305**, 006 (2003) U. Chattapadhyay, A. Corsetti and P. Nath, Phys. Rev. D **68**, 035005 (2003); A. Lahanas and D. V. Nanop oulos, Phys. Lett. B **568** 55 (2003); A. Djouadi, M. Drees and J. L. Kneur, JHEP **0603**, 033 (2006).

[23] SUGRA Working Group Collaboration (S. Abel et. al.), hep-ph/0003154.

[24] For a review see,e.g., Higgs boson theory and phenomenology. Marcela Carena (Fermilab) , Howard E. Haber (UC, Santa Cruz) . FERMILAB-PUB-02-114-T, SCIPP-02-07, Aug 2002. 87pp. Published in Prog.Part.Nucl.Phys.50:63-152,2003. e-Print: hep-ph/0208209 (review)

[25] http://lepsusy.web.cern.ch/lepsusy/www/lspmsugra_summer02/02-06.2/mSUGRA_208.html

[26] V. A. Bednyakov, S. G. Kovalenko, H. V. Klapdor-Kleingrothaus and Y. Ramachers, Z. Phys. A **357**, 339 (1997); V. A. Bednyakov, H. V. Klapdor-Kleingrothaus and S. G. Kovalenko, Phys. Rev. D **55**, 503 (1997); A. Bottino, F. Donato, N. Fornengo and S. Scopel, Phys. Rev. D **63**, 125003 (2001); J. R. Ellis, K. A. Olive, Y. Santoso and V. C. Spanos, Phys. Rev. D **69**, 015005 (2004); V. A. Bednyakov and H. V. Klapdor-Kleingrothaus, Phys. Rev. D **70**, 096006 (2004); L. Calibbi, Y. Mambrini and S. K. Vempati, arXiv:0704.3518 [hep-ph].

[27] L. S. Stark, P. Hafliger, A. Biland and F. Pauss, JHEP **0508**, 059 (2005) [arXiv:hep-ph/0502197]. See also Djouadi et al in [22]

[28] J.M. Frere, D.R.T. Jones and S. Raby, Nucl. Phys. B **222**, 11 (1983); J. A. Casas, A. Lleyda and C. Munoz, Nucl. Phys. B **471**, 3 (1996) [arXiv:hep-ph/9507294].

[29] S. Chen, et al., CLEO Collaboration, Phys. Rev. Lett. **87**, 251807 (2001), hep-ex/0108032; P. Koppenburg *et al.* [Belle Collaboration], Phys. Rev. Lett. **93**, 061803 (2004) B. Aubert, et al., BaBar Collaboration, hep-ex/0207076.

[30] K. i. Okumura and L. Roszkowski, Phys. Rev. Lett. **92**, 161801 (2004); M. E. Gomez, T. Ibrahim, P. Nath and S. Skadhauge, Phys. Rev. D **74**, 015015 (2006).

[31] See,e.g., M. Claudson, I. J. Hall, I. I. Hinchliffe, Nucl. Phys. B **228**, 501 (1983); A. Kusenko, P. Langacker, G. Segre, Phys. Rev. D **54**, 5824 (1996).

[32] A. Djouadi, J. L. Kneur and G. Moultaka, Comput. Phys. Commun. **176**, 426 (2007), [arXiv:hep-ph/0211331].

[33] G. Belanger, F. Boudjema, A. Pukhov and A. Semenov, Comput. Phys. Commun. **176**, 367 (2007) [arXiv:hep-ph/0607059].

[34] S. Heinemeyer, W. Hollik and G. Weiglein, Phys. Rep. **425**, 265 (2006), hep-ph/0412214.

[35] S. Heinemeyer, hep-ph/0408340.

[36] S. Heinemeyer, Int. J. Mod. Phys. A **21**, 2659 (2006).

[37] G. Dedgassi, S. Heinemeyer, W. Hollik, P. Slavich and G. Weiglein, Eur. Phys. J. C **28**, 133 (2003), hep-ph/0212020.

[38] B. Allanach, A. Djouadi, J. Kneur, W. Porod and P. Slavich, J. High Energy Phys. **0409**, 044 (2004), hep-ph/0406166.

[39] R. Demina, J. D. Lykken and K. T. Matchev, Phys. Rev. D **62**, 035011 (2000).

[40] C. Boehm, A. Djouadi and Y. Mambrini, Phys. Rev. D **61**, 095006 (2000).

[41] S. P. Das, A. Datta and M. Guchait, Phys. Rev. D **65**, 095006 (2002); S. P. Das, A. Datta and M. Maity, Phys. Lett. B **596**, 293 (2004).

[42] T. Sjostrand, P. Eden, C. Friberg, L. Lonnblad, G. Miu, S. Mrenna and E. Norrbin, Comp. Phys. Comm. **135**, 238 (2001); For a more recent version see, JHEP **0605**, 026 (2006)

[43] See, *e.g.* , A.Pukhov, CalcHEP−a package for evaluation of Feynman diagrams and integration over multi-particle phase space (hep-ph/9908288). For the more recent versions see: http://www.ifh.de/pukhov/calchep.html.

[44] ATLAS, Detector and physics performance, Technical design report, Vol II, CERN/LHCC/99-15.

[45] CMS physics, technical design report, vol-1.

[46] K. Grassie and P. N. Pandita, Phys. Rev. D **30**, 22 (1984).

[47] Amitava Datta, Aseshkrishna Datta and S. Raychaudhuri, Phys. Lett. B **349**, 113 (1995), Eur. Phys. J. C**1**, 375 (1998).

[48] Amitava Datta and Asesh Krishna Datta, Phys. Lett. B **578**, 165 (2004).